ORIGINAL ARTICLE

Assessment of seasonal variation of saltwater intrusion using integrated geophysical and hydrochemical methods in some selected part of Ogun Waterside, Southwest, Nigeria

Ganiyu Olabode Badmus[1,5] · Olukayode Dewunmi Akinyemi[2,5] · Adewole Michael Gbadebo[3,5] · John Adebayo Oyedepo[4,5] · Gbolahan Muyiwa Folarin[5]

Abstract

This study presents the seasonal variation of saltwater intrusion in Ogun Waterside using a combine electrical resistivity tomography (ERT) and groundwater physicochemical analysis. The ERT survey was completed with 22 profiles using dipole–dipole array method covering seven major communities (Imakun-omi, Irokun, Isekun, Ode-omi, Iwopin, Itebu-elero, and Ayila) east of Lagos. The field survey was carried out between August 2016 and March 2017 with a minimum electrode spacing of 2.5 m. The inverted model generally revealed a resistivity range of 1.0 Ωm–100,000 Ωm delineated through a depth range of 37 m–197 m. The model obtained for Imakun-omi, Irokun, Isekun, and Ode-omi revealed significant impact of saltwater intrusion from nearby lagoon, sea, or creeks indicated as low-resistivity structures generally below 20 Ωm. The intrusion is more pronounced during the dry season due to decrease in groundwater level associated with low precipitation and possibly aggravated by high rate of groundwater extraction. Groundwater physicochemical analysis obtained in the study area revealed a general increase in the ionic concentrations with a corresponding increase in the water quality index (WQI) during dry season. The calculated WQI for the wet and dry seasons revealed good-to-excellent water quality in most samples taken in the study area except for samples taken in the southern part which were found within the poor-to-very poor water quality category. Evidence from the physicochemical analysis of groundwater samples corroborates the ERT result viz-a-viz the aquifer contamination status of Imakun-omi, Irokun, Isekun, and Ode-omi.

Keywords Saline water · Pollution · Geoelectric layer · Coastal aquifer · 2-D ERT models

✉ Ganiyu Olabode Badmus
  ogbadmus@abuad.edu.ng

1 Department of Mathematical and Physical Sciences, Afe Babalola University, P.M.B. 5454, Ado-Ekiti, Nigeria

2 Department of Physics, Federal University of Agriculture, P.M.B. 2240, Abeokuta, Nigeria

3 Department of Environmental Management and Toxicology, Federal University of Agriculture, P.M.B. 2240, Abeokuta, Nigeria

4 Institute of Food Security, Environmental Resources and Agricultural Research, Federal University of Agriculture, P.M.B. 2240, Abeokuta, Nigeria

5 Centre of Excellence in Agricultural Development and Sustainable Environment, Federal University of Agriculture, P.M.B. 2240, Abeokuta, Nigeria

Introduction

Freshwater quality and its accessibility are one of the essential environmental and sustainability issues of the twenty-first century. Since groundwater represents more than 90% of the accessible freshwater resources, it can be seen as the largest reservoir of freshwater readily available to humans. Groundwater became the primary source of freshwater in many African countries including Nigeria owing to the fact that government gives less importance to building of dams to produce potable water for public use (Adeyemo et al. 2017). This perhaps led to the uncontrolled siting of boreholes by many Nigerians.

Coastal dwellers within 100 km of the coast represent about 37% of the global population. In developing nations, coastal zones form the centre of attention for economic activity and human settlement. The major occupation providing income for a large percentage of coastal dwellers is

agriculture which largely relies on groundwater as the primary source of freshwater to survive. Therefore, continuous increase in population of coastal inhabitant could lead to groundwater over-exploitation which may in turn put the natural ecosystem under intense pressure.

Coastal region presents an active zone where saline water interacts with fresh groundwater in the coastal aquifers (Goebel et al. 2017). Under normal condition, freshwater naturally flows towards the sea, but over-abstraction may result in the inversion of the groundwater flow from the sea towards the inland causing migration of saline water into aquifers that are hydraulically connected with the sea (Nowroozi et al. 1999; Abdalla et al. 2010; Abd-Elhamid et al. 2015). Therefore, sustainable extraction of water from coastal aquifers is essential to control saltwater intrusion to maintain a long-term freshwater supply (Darnault and Godinez 2008).

The coastal areas in the Nigerian provinces are liable to groundwater overdraft as a result of its growing population and the associated agricultural activities and consequently, to an increase threat of saltwater intrusion. Several authors (Adepelumi et al. 2009; Oyedele and Momoh 2009; Adeoti et al. 2010; Aizebeokhai 2010; Adebo 2012; Ayolabi et al. 2013b; Oyeyemi et al. 2015; Adeyemo et al. 2015) have carried out a number of studies on saline water intrusion in the southwestern coastal zones of Nigeria, particularly within Lagos and Ondo state. However, very few related studies have been reportedly done on the coastal aquifer of Ogun Waterside (Fig. 1).

This study aims to assess the seasonal variation of saltwater intrusion using integrated geophysical and hydrochemical methods with the objective of delineating the vertical and lateral degree of saltwater intrusion in some selected part of Ogun Waterside.

Site description and geology

The site under investigation is Ogun Waterside in the eastern flank of Ogun state, southwestern Nigeria. The area share borders with Ijebu East Local Government in the west, Lagos State towards the south, and Ondo State in the north. Geographically, not less than half of the length of the study site is encircled with water which extends from Ondo State to Lagos State (Odebiyi et al. 2013). This feature primarily gave birth to the choice of the name Waterside given by the Government. The area is very much connected with other maritime states of southwestern Nigeria
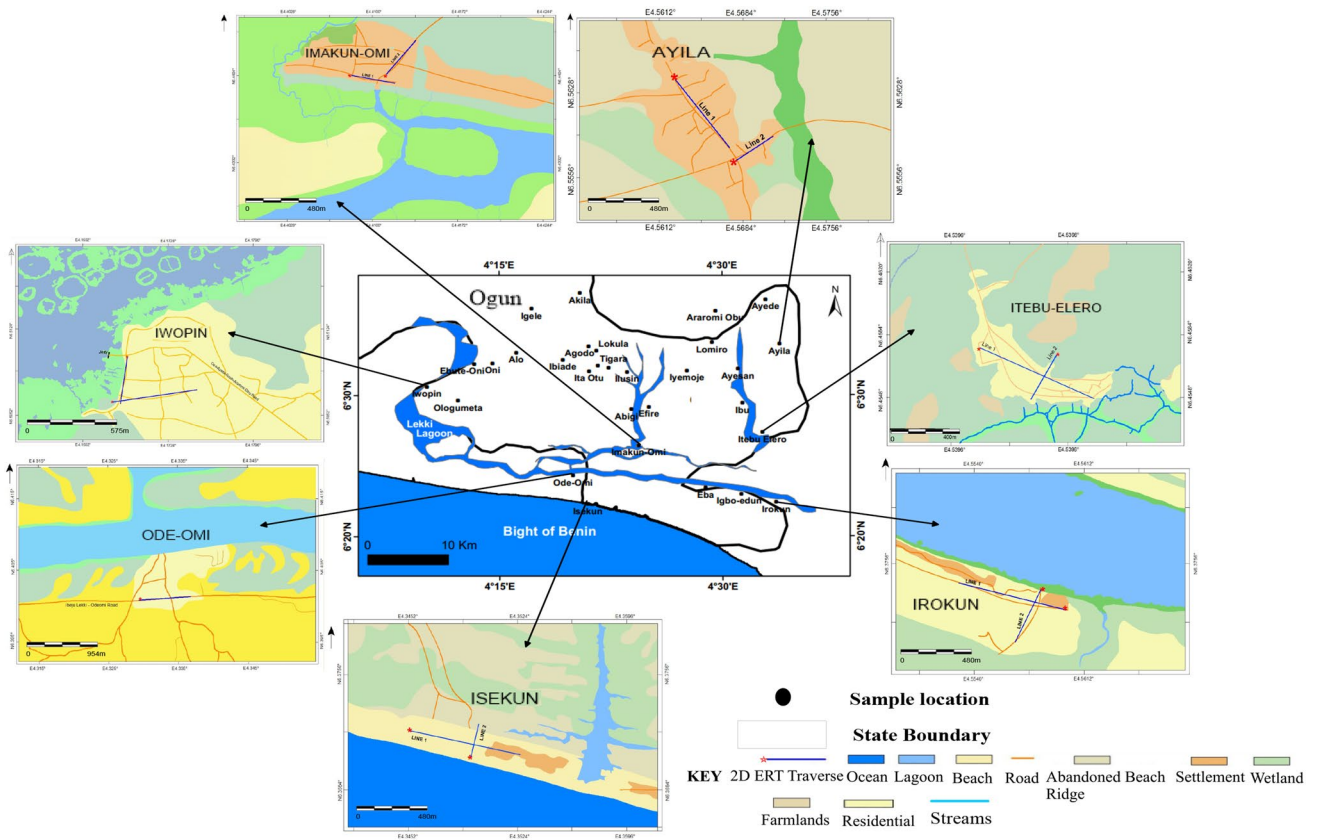

Fig. 1 Location map of Ogun Waterside showing ERT lines and sampling points

and extends approximately 1000 km^2 along the Bight of Benin. It is bounded by latitudes $6°18'N - 6°40'N$ and longitudes $4°6'E - 4°38'E$, and has a population of 72,935 at the 2006 census (Idowu et al. 2012). With a population growth rate of 3.35%, Ogun Waterside population is projected to be approximately 140,000 in 2025. The climate in Ogun Waterside can be defined with two different seasons: the dry season usually between December and March, and the wet season between April and November. The variation in monthly temperature ranges from 32 °C in February to 23 °C in July, while the mean annual rainfall is about 1300 mm. The southern region of the study area is mainly of mangrove swamp, while the northern flank is blessed with derived Savannah vegetation and the central part falls in the rainforest belt. Ogun Waterside has fertile land rich in organic matter which makes it support cultivation of various agricultural produce such as oil palm, rice, maize, cassava, yam, and rubber (Olaoye et al. 2012).

Ogun Waterside lies within the Nigerian section of the Dahomey basin which spans through the seashore of Ghana, Togo, Republic of Benin, and Nigeria. The basin originated from rifting during the Jurassic-to-early Cretaceous era (Omatsola and Adegoke 1981). The basin is lithologically composed of alternation of sands and clays with shale and limestone intercalation (Jones and Hockey 1964). The stratigraphic studies of the Dahomey Basin revealed six lithostratigraphic Formations identified as: Abeokuta group, Ewekoro Formation, Akinbo Formation, Oshosun Formation, Ilaro Formation, and the Benin Formation (Billman 1992; Fakolade and Obasi 2012; Olabode 2015).

The Benin Formation (Coastal Plain Sands and Alluvium) comprises of poorly sorted sands with lenses of clay (Adeyemo et al. 2015), and it occupies more than 80% of the study area covering the southern, western, central, eastern, and part of the northern flank (Fig. 2). The formation is permeable and consists of multi-layered aquifer units separated by clayey/silty layer. The most resent sediments present an unconfined (phreatic) aquifer which is exploited by shallow bore wells and dug wells (Ayolabi et al. 2013c). The Abeokuta Group (sand, clay, and shale), Ewekoro/Akinbo Formation (shale and limestone), and Ilaro Formation (sandstone and limestone) trend towards the northern part of the study area. The aquifer is primarily recharge through infiltration from precipitated rain water and discharge by groundwater extraction, flow into the River and evapotranspiration. Readers may refer to Obaje (2009) for the detailed lithostratigraphic succession of the Dahomey Basin.
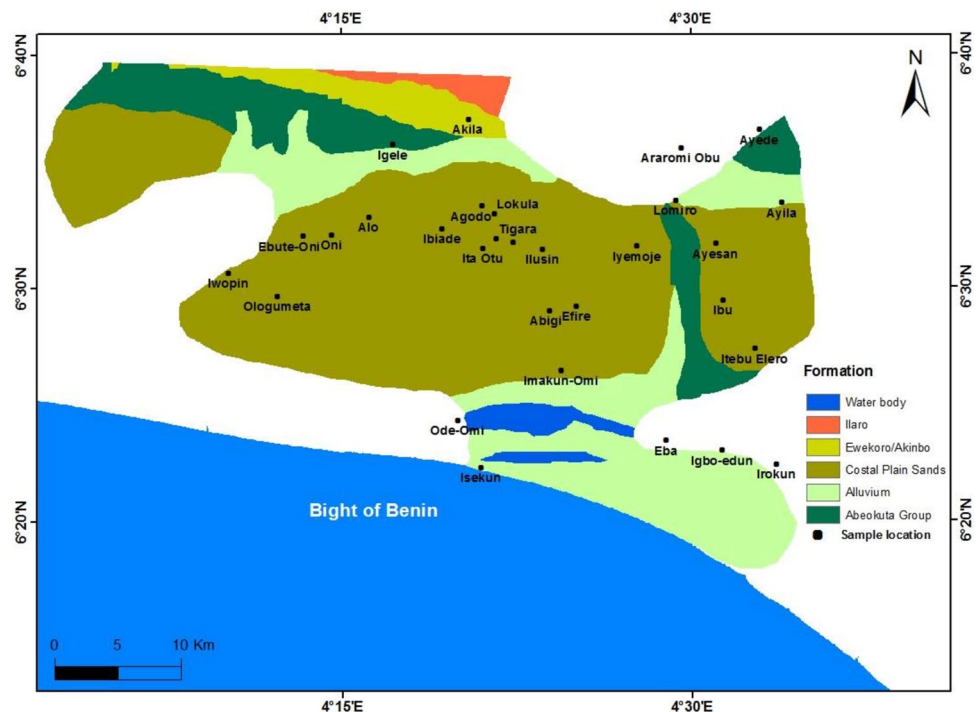
Methodology

Integrated geophysical and hydrochemical methods were employed for this study.

Geophysical data acquisition and analysis

Electrical Resistivity Tomography (ERT) survey using AGI SuperSting R8/IP Earth Resistivity meter with inbuilt

Fig. 2 Geology map of Ogun Waterside

processor for 112 multi-electrode system was carried out in Ogun Waterside. Field survey was done in August 2016 (wet season) and the survey was repeated in March 2017 (dry season) to achieve the aim of this research work. The resistivity survey was completed with twenty six (26) 2-D ERT profiles. Dipole–dipole array technique was employed for this study because of its high resolution and multi-channel capability. Field investigation was done with a minimum electrode separation of 2.5 m and a maximum of 10 m as a result of constrain in space, since some part of the study area are not accessible. Thus, the maximum length of array for this study is 1120 m. The acquired ERT data were inverted using Earth Imager software. The software modeled the bulk data into several cells of which each contains a number of records (Ayolabi et al. 2013a). The calculated resistivity in each cell was used to produce the apparent resistivity pseudo-section with which actual resistivity measurement was compared and the difference in measurement was specified by the root-mean-square error (AGI 2003).

Physicochemical analysis

Thirty groundwater samples (17 boreholes, 13 dug wells) were taken from different sampling points within Ogun Waterside during the month of August 2016 and March 2017. The specific locations of studied boreholes and dug wells were taken with Global Positioning System (GARMIN GPS 72H). The groundwater samples were collected in a litre plastic container for analysis. Sampling was done in accordance with the standards outlined by APHA (1995). Some water quality parameters such as pH, Total Dissolved Solids (TDS), and Electrical Conductivity (EC) were determined in-situ using a hand-held digital meter (Jenway 430) calibrated with pH solution 7 to preserve accuracy. Analysis of the major anions and cations were done in the laboratory of the Institute of Agricultural Research and Training (IAR&T), Ibadan. The analyzed parameters include bicarbonate, potassium, sodium, calcium, sulphate, chloride, and nitrate. Analytical results were further compared with recommended standards specified for drinking by the Nigerian Standard for Drinking Water Quality (NSDWQ 2007) and the Water Quality Index (WQI) was determined using the below steps proposed by Batabyal and Chakraborty (2015):

1. Each of the analyzed parameters was allotted a weight (w_i) between 1 and 5 based on its importance in influencing groundwater quality. The least important parameter was allotted the minimal weight of 1, while the maximal weight of 5 was allotted to the most important parameter.

2. The relative weight (W_i) of the analyzed parameter was computed with Eq. 1:

$$W_i = \frac{w_i}{\sum_{i=1}^{n} w_i}. \tag{1}$$

3. The concentration (C_i) of each parameter in each sample was divided with its prescribed standard (S_i) proposed by NSDWQ guidelines and the result is multiplied by 100 to estimate the quality rating scale (q_i) as seen in Eq. 2:

$$q_i = \left(\frac{C_i}{S_i} \right) \times 100. \tag{2}$$

4. The sub index (SI_i) is evaluated for each parameter using Eq. 3:

$$SI_i = W_i \times q_i. \tag{3}$$

5. The water quality index for each sample is finally evaluated using Eq. 4:

$$WQI = \sum_{i=1}^{n} SI_i. \tag{4}$$

The computed WQI values were classified into four categories according to Table 1, and the water quality distribution map of Ogun Waterside was contour with surfer 12 using kriging as the interpolation method.

Results and discussion

Analysis of electrical resistivity tomography

A total of twenty six (26) 2D ERT lines were laid, four (4) ERT data (line 1 in Irokun and Ayila) were very noisy as a possible result of poor electrode contact and consequently were not interpretable. The obtained data were processed and inverted into 2-D ERT models with lateral extent ranging from 240 to 1120 m, and vertical extent of 37 m–197 m. The inverted model generally revealed three geoelectric layers with layer resistivity values varying from 5.6 to 100,000 Ωm, 1.0 Ωm–100,000 Ωm, and 19 Ωm–4227 Ωm in the topsoil, second, and third geoelectric layers, respectively. The inverted 2-D sections revealed variance in subsurface

Table 1 Water quality index range/water quality category (modified after Batabyal and Chakraborty 2015)

Water quality index range	Water category
0–50	Excellent water
50–100	Good water
100–200	Poor water
200–300	Very poor (unsuitable for drinking)

resistivity which evidently reflected different fluid content and lithology (sand, clay, and sandy clay/clayey sand). The aquifer units are found within the sand and sandy clay/clayey layer with variation in groundwater yield. Some of the aquifer units in the study area reflected the impact of brackish/saltwater intrusion from nearby lagoon, sea, or creek, and are characterized by low-resistivity values.

The 2D electrical resistivity sections for line 1 during wet and dry seasons in Imakun-omi are presented as resistivity–depth structures in Fig. 3a. The geoelectric image showed variation in resistivity distribution with electrical resistivity values ranging from 7.6 to 10,000 Ωm probing a depth of 99 m during wet season and from 7.8 to 10,000 Ωm probing a depth of 59 m during dry season. The low-resistivity (< 20 Ωm) structure delineated between the lateral position 160 m–400 m at depth range of 8 m–59 m during the dry season is reflective of possible brackish water invasion from the lagoon. The isolated pockets of high resistivity values (677 Ωm–1662 Ωm) found between the lateral position 308 m–352 m and 372 m–420 m are suggestive of sand saturated with freshwater.

Figure 3b shows the 2D electrical resistivity sections for line 2 during wet and dry seasons in Imakun-omi. The ground surface below this section from surface positions 60 m–260 m just beneath the sandy topsoil revealed low-resistivity values (< 20 Ωm) suggestive of possible brackish

water pollution from nearby creek at a near surface depth of 8 m–84 m and lateral distances of 50 m–260 m during wet season. This is more evident during the dry season, which revealed that most part of the geoelectric layer has been invaded by brackish water spanning through lateral distances of 1.0 m–480 m to a depth of 98 m.

The 2D electrical resistivity sections for line 2 during wet and dry season in Irokun are presented in Fig. 3c. The subsurface within the second geoelectric layer in this traverse is composed predominantly of low-resistivity (< 10 Ωm) structure reflective of saline water intrusion from the lagoon. It was evident in the dry season that a penetrative conduit suspected to be a fault has breached the freshwater aquifer zone between electrode positions 235 m–285 m. This conduit allows saltwater to migrate upward (up-coning) into the overlying freshwater aquifer which later spreads through a lateral distance of about 160 m within the second geoelectric layer in the wet season, but covers almost the entire traverse line in the dry season. This suggests that saline water is progressively migrating inter land in this region.

Figure 3d shows the 2D electrical resistivity sections for line 1 during wet and dry seasons in Isekun. The first geoelectric layer is composed of beach sand and is the region with the shallow aquifer that straddled above the denser saline region where most hand dug wells source groundwater. The second geoelectric layer in this traverse is composed
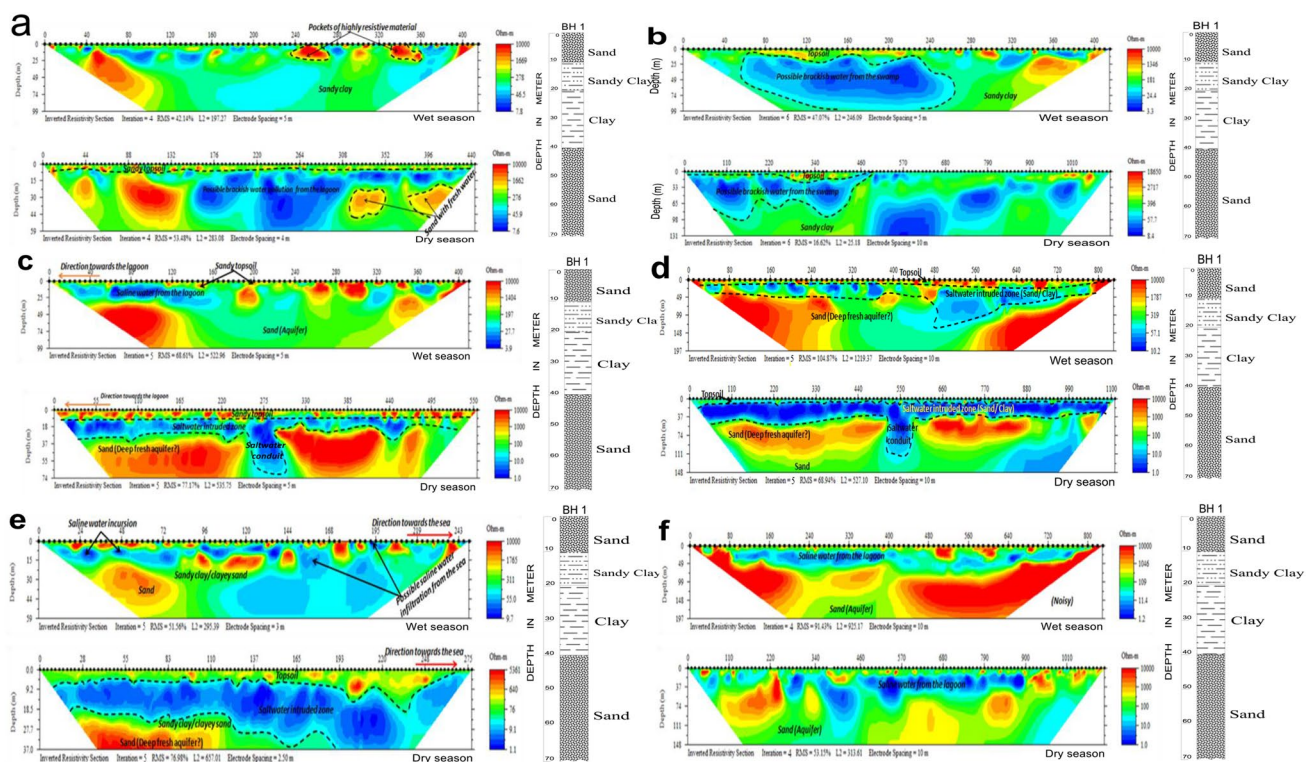

Fig. 3 Inverted 2-D resistivity tomography sections in (**a**,**b**) Imakun-omi, (**c**) Irokun, (**d**,**e**) Isekun, and (**f**) Ode-omi

preponderantly of low-resistivity (< 20 Ωm) signature suggestive of brackish/saline water intrusion from the sea. This is more evident during the dry season which shows that the whole geoelectric layer has been completely affected by saline water intrusion to a depth of 110 m beneath electrode position 550 m. This can be ascribed to a suspected saltwater flow conduit which coincides with the observed stream that terminates at the beach. The third geoelectric layer revealed moderate-to-high electrical resistivity signature suggestive of sand layer which represents deep freshwater aquifer within the investigated region.

Figure 3e presents the 2D electrical resistivity sections along line 2 during wet and dry seasons in Isekun. The first geoelectric layer is composed of beach sand with the shallow aquifer that straddled above the denser saline region where most hand dug wells source groundwater within this region. The second geoelectric layer comprised low-resistivity signature (< 20 Ωm) reflective of brackish/saline water intrusion from the sea. This is more evident during the dry season which shows that the entire geoelectric layer has been impacted by seawater intrusion to a depth of 37 m below the surface. The third geoelectric layer revealed electrical resistivity range of 55 Ωm–1765 Ωm during wet season and 26 Ωm–220 Ωm during dry season, suggestive of sandy clay/clayey sand layer. High electrical resistivity signature

noticed at the bottom left-hand side of the profiles is suggestive of sand which represents deep freshwater aquifer unit within the investigated region, possibly protected from saline water contamination by the overlying thin clayey layer.

Figure 3f presents the electrical resistivity tomography sections obtained for wet and dry seasons in Ode-omi. The topmost layer is characterized by low-to-high electrical resistivity structure. Directly underlying this layer is a successive layer of low-resistivity (< 20 Ωm) structure suggestive of possible brackish water intrusion from the lagoon and is discontinuous in lateral extent.

The 2D electrical resistivity sections for line 1 during the wet and dry seasons in Iwopin are presented in Fig. 4a. The first geoelectric layer was delineated to a maximum depth of about 11 m for the two seasons. This layer revealed sandy clay/clayey sand which constitute the shallow aquifer overlying the lateritic soil/sand layer. The second geoelectric layer is represented by low-to-high electrical resistivity signature, delineated within the depth range of 33 m–44 m and 46 m–71 m for the wet and dry seasons, respectively. The low-resistivity structure present at a depth of about 12 m below the topsoil between the lateral distances of 245 m–360 m in the wet season is suggestive of clay/peat. The relatively high resistivity values obtained at same lateral distances and depth during dry season revealed dry lateritic
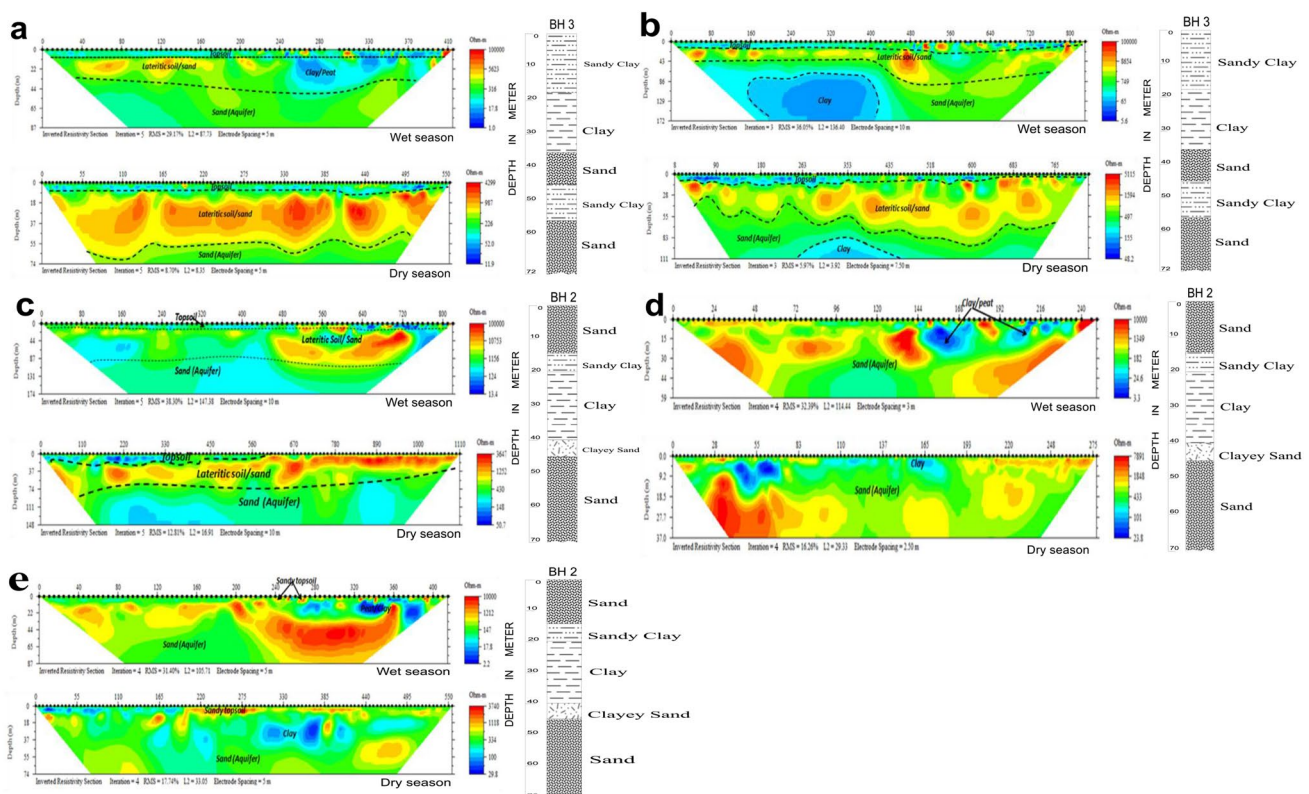

Fig. 4 Inverted 2-D resistivity tomography sections in (**a**, **b**) Iwopin, (**c,d**) Itebu-elero, and (**e**) Ayila

soil/sandy clay in water saturated condition during wet season, but dried up during the dry season. The third geoelectric layer has electrical resistivity range of 25 Ωm–1335 Ωm, delineated to a depth of about 87 m during the wet season and a resistivity range of 108 Ωm–472 Ωm, and delineated to a depth of about 74 m during the dry season. This is suggestive of sand layer which represents deep freshwater aquifer unit that can be exploited by deep boreholes within the investigated region.

The 2D electrical resistivity sections for line 2 during wet and dry seasons in Iwopin are presented in Fig. 4b. The first geoelectric layer represents the topsoil with varying electrical resistivity range of 5.6 Ωm–29,418 Ωm, delineated to a depth range of 10 m–22 m during the wet season and a resistivity range of 42.8 Ωm–497 Ωm, and delineated to a depth range of about 2 m–16 m during the dry season. This region comprised sandy clay/clayey sand with some pockets of highly resistive soil. The second geoelectric layer is predominantly represented by high electrical resistivity signature range of 749 Ωm–54,238 Ωm, delineated within the depth range of 43 m–97 m during the wet season and a resistivity range of 497 Ωm–2855 Ωm, and delineated within the depth range of 42 m–97 m during the dry season. The high electrical resistivity signature in this region is suggestive of lateritic soil/sand. The third geoelectric layer is represented with electrical resistivity range of 19 Ωm–749 Ωm during the wet season and 155 Ωm–453 Ωm during the dry season, and is suggestive of sand layer. This represents deep aquifer unit delineated to a depth of about 172 m and 111 m for the wet and dry seasons, respectively. The low-resistivity structure present at a depth range of about 64 m–172 m between the lateral distances of 160 m–400 m in the wet season revealed the presence of clay. The relatively high resistivity values obtained at same lateral distances and depth during dry season revealed the presence of compacted clay in water saturated condition during wet season.

The 2D electrical resistivity sections for line 1 during wet and dry seasons in Itebu-elero are presented in Fig. 4c. The subsurface within this region showed similar trend for the wet and the dry season data sets, having near surface low-resistivity structure indicative of clay/peat within the topsoil. The presence of high resistivity structure (above 5000 Ω-m) in the second layer is suggestive of possible presence of high-quality freshwater aquifer or presence of sandy/lateritic materials; while the third layer is suggestive of sand layer which represents deep aquifer unit that can be exploited by deep boreholes.

The 2D electrical resistivity sections for line 2 during wet and dry seasons in Itebu-elero are presented in Fig. 4d. The subsurface within this region is dominated by moderately high resistivity structure reflective of freshwater aquifer and also revealed isolated near surface low-resistivity structure reflective of clay/peat.

The 2D electrical resistivity sections for line 2 during wet and dry seasons in Ayila are presented in Fig. 4e. The geoelectric image showed variation in resistivity distribution with electrical resistivity values varying from 2.2 to 10,000 Ωm probing a depth of 87 m during the wet season and from 29.8 to 3740 Ωm probing a depth of 74 m during the dry season. The ground surface within this region is composed of moderately high resistivity structure reflective of freshwater aquifer or presence of sandy/lateritic materials. Isolated low-resistivity (below 50 Ωm) structure found beneath the sandy clay topsoil at a lateral distance between 280 and 385 m is reflective of clay/peat.

The modes of saltwater intrusion as evident from the above interpreted 2D sections are lateral intrusion from nearby lagoon, sea, or creek and up-coning from a deeper saline zone due to differential pressure gradient. The major factors thought to be responsible for the observed saltwater intrusion in the study area are: (1) groundwater over-abstraction which has resulted in the inversion of groundwater flow from the lagoon, sea, or creek towards the inland, and (2) the occurrence of brackish/saline water trapped by low-permeability sediment of marine origin during Quaternary age.

Correlation of borehole lithology with ERT imaging

The lithologies of the three boreholes drilled at Imakun-omi, Abigi, and Iwopin are presented in Fig. 5. Sand and clay dominate the major part of the study area. Since clay has low resistivity, it could be difficult to identify layers that contain saltwater within the clay formation which may contain freshwater. Hence, the resistivity interpretation of saltwater and freshwater aquifers can be more dependable if supported by a more reliable geophysical anomaly, capable of resolving the two aquifers more competently (Gurunadha Rao et al. 2011). However, a comparative analysis of resistivity profile data and borehole log data can be used to resolve this ambiguity (Hodlur et al. 2010).

Comparisons of the depth inversion sections of Imakun-omi, Irokun, Isekun, and Ode-omi with the borehole lithology of BH1 suggest that there are good agreements. Generally, the first geoelectric layer of the profiles up to about 10 m was observed to represent the sandy topsoil. The second layer encountered between 10 and about 37 m suggests a sandy clay/clay formation saturated with saltwater. The third layer up to a depth of about 197 m in Isekun was basically sandy clay formation/medium grained sand. Comparison of the resistivity section of Iwopin with the borehole lithology of BH3 showed that the top layer up to 11 m depth represents sandy clay formation. Further below the sandy clay formation, lateritic soil/sandy clay up to about 100 m depth was reported. The third layer represents medium grain sand formation up to 87 m depth. The ERT sections of Itebu-elero also agree with the borehole lithology of BH2.
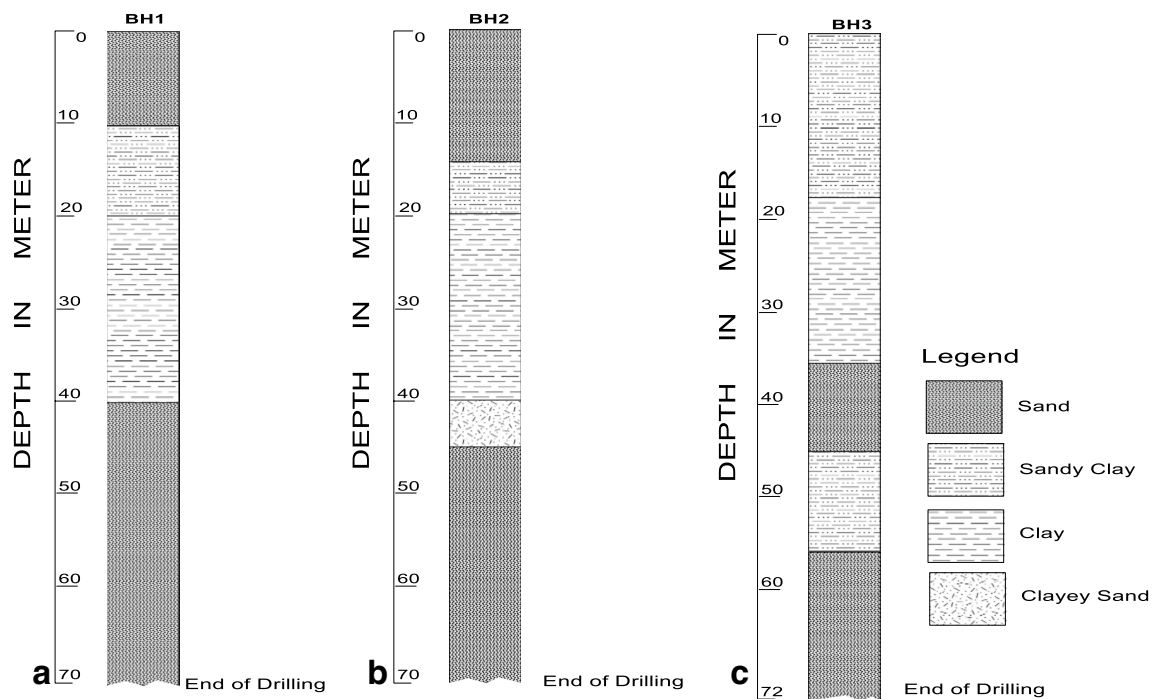
Fig. 5 Borehole logs used to juxtapose the inverted ERT sections (**a**) borehole drilled in Imakun-omi (**b**) borehole drilled in Abigi, and (**c**) borehole drilled in Iwopin

Physicochemical analysis

Tables 2 and 3 present the result of the physicochemical analysis of the groundwater samples carried out during wet season (August 2016) and dry season (March 2017), respectively. The concentrations of the analyzed parameters were further compared with the prescribed standard proposed by the NSDWQ (2007). The pH value of the sampled water ranges from 6.63 to 7.50 in August 2016 and 4.68–7.19 in March 2017, with a mean value decreasing from 6.82 to 5.96 with difference of 0.86 (14.43%). The mean concentrations of the TDS increased from 429.58 mg/L during the wet season to 527.78 mg/L in the dry season, with a difference of 98.2 (22.86%). The TDS values exceeded the permissible limits of 500 mg/L proposed by NSDWQ in about 17% of the groundwater sample in the wet season and 20% during dry season (Fig. 6a). EC values were found to be relatively higher than the prescribed limit of 1000 μS/cm for portable water in about 10% of the sampled water during wet season and 17% in dry season (Fig. 6b). Potassium, sodium, calcium, magnesium, bicarbonate, and sulphate concentrations exist within the permissible limit specified by NSDWQ. However, the mean chloride values increased from 176.37 mg/L in the wet season to 276.09 mg/L in the dry season, with an

interval difference of 99.72 (56.54%). About 13% of the groundwater samples were identified to have chloride concentration in excess of the allowable limits of 250 mg/L set by NSDWQ (2007) (Fig. 6c). Generally, the analytical result shows an increase in ionic concentrations in dry season when compared with the wet season analysis. High concentration of TDS, EC, and Cl noticed in samples taken from Imakun-omi, Isekun, Irokun, and Ode-omi may be an indication of saltwater intrusion from the nearby creek, sea, or lagoon.

The WQI values range from 35.19 to 141.72 in the wet season and from 38.6 to 266.79 in the dry season (Table 4). About 63.33% of the samples were considered excellent during the wet season, 33.33% were considered good, and 3.33% were identified to be poor, while during the dry season, 53.33% of the sampled water were excellent, about 36.37% were good, 6.67% were poor, and 3.33% were identified to be very poor (unsuitable for drinking). The WQI map presented in Fig. 7 revealed that the samples taken around the southern part of Ogun Waterside show signs of deterioration as it ranges from good to poor water type in the wet season, while the dry season samples vary from poor to very poor water type. This deterioration may have resulted from the migration of saltwater from nearby creek, sea, or lagoon towards the coastal groundwater aquifer in the southern

Table 2 Results of the physical and chemical contents of groundwater sample analyzed for the wet season (modified after Badmus et al. 2020, p. 3)

Sample no.	Sample location	Source type	pH	EC	TDS	Na$^+$	K$^+$	Mg^{2+}	Ca^{2+}	Cl$^-$	SO$_4{}^{2-}$	HCO$_3{}^-$
S-1	Ilusin	BW	6.80	617.77	395.37	37.40	64.65	2.60	2.12	106.30	1.80	180.50
S-2	Ibiade	DW	6.73	1118.48	715.83	35.83	61.77	2.40	2.11	142.00	1.82	469.90
S-3	Oni	BW	6.63	493.58	315.89	34.13	60.75	2.45	1.93	71.00	1.23	144.40
S-4	Ebute-Oni	DW	6.83	665.58	425.97	34.85	62.15	2.40	3.11	177.45	1.61	144.40
S-5	Ologumeta	DW	6.80	445.13	284.88	35.73	62.85	1.92	2.95	35.50	1.73	144.20
S-6	Iwopin	DW	6.73	712.30	455.87	30.45	60.82	2.78	2.82	213.00	1.60	144.40
S-7	Alo	BW	6.88	617.97	395.50	41.55	60.80	2.74	2.74	177.65	1.62	108.40
S-8	Igele	BW	6.85	505.59	323.58	40.85	62.75	1.73	1.84	106.50	1.51	108.40
S-9	Akila	BW	6.80	573.64	367.13	40.40	62.75	2.83	4.45	106.65	5.65	144.40
S-10	Agodo	DW	6.83	606.00	387.84	42.18	51.20	2.73	3.70	142.00	1.43	144.60
S-11	Lokula	BW	6.80	505.88	323.76	46.25	55.30	2.73	2.92	106.56	1.60	108.40
S-12	Igbafowo	BW	6.70	488.75	312.80	41.25	48.50	2.60	3.30	71.00	1.75	144.40
S-13	Abigi	BW	6.80	397.44	254.36	42.50	60.45	2.40	3.25	35.65	1.71	108.40
S-14	Araromi Obu	BW	6.90	612.64	392.09	41.80	57.80	1.92	2.82	177.50	1.85	108.40
S-15	Ayede	BW	7.05	679.70	435.01	43.20	60.75	2.60	2.85	71.50	1.71	252.40
S-16	Ayila	BW	7.50	664.97	425.58	40.60	58.65	1.45	2.58	248.30	1.60	72.40
S-17	Itebu Elero	DW	6.83	530.08	339.25	51.50	62.55	2.61	2.44	71.00	4.75	144.40
S-18	Ayesan	DW	6.82	534.75	342.24	53.25	64.60	2.48	2.70	142.00	4.91	72.30
S-19	Lomiro	BW	6.73	880.34	563.42	35.55	54.20	2.30	2.63	177.40	2.74	288.60
S-20	Ibu	BW	6.83	635.36	406.63	31.55	46.30	2.74	2.41	177.50	1.93	144.20
S-21	Iyemoje	DW	6.73	511.02	327.05	48.91	53.35	2.44	2.34	71.00	4.61	144.40
S-22	Efire	BW	6.75	415.88	266.16	34.80	44.81	2.60	2.45	71.35	1.75	108.40
S-23	Imakun-Omi	BW	6.80	2021.33	1293.65	51.00	58.40	2.65	2.55	994.00	4.55	180.50
S-24	Ita Otu	BW	6.85	531.91	340.42	35.45	47.15	2.64	2.41	106.50	1.87	144.40
S-25	Tigara	BW	6.80	446.83	285.97	41.10	60.56	1.71	2.15	106.50	1.55	72.40
S-26	Irokun	DW	6.73	941.61	602.63	38.80	58.55	1.47	1.93	319.75	1.53	180.60
S-27	Igbo-edun	DW	6.85	560.03	358.42	41.65	60.49	2.46	1.81	142.00	1.61	108.40
S-28	Eba	DW	6.75	434.75	278.24	37.15	55.75	1.93	2.11	71.25	1.45	108.60
S-29	Isekun	DW	6.80	1154.77	739.05	36.55	56.10	1.88	1.97	532.60	1.45	108.50
S-30	Ode-Omi	DW	6.78	832.63	532.88	41.55	58.20	1.91	1.76	319.55	1.51	108.40
S_i	–	–	8.5	1,000	500	200	–	0.2	–	250	100	–
Min	–	–	6.63	346.84	254.36	30.45	44.81	1.45	1.76	35.50	1.23	72.30
Max	–	–	7.50	2021.33	1293.65	53.25	64.65	2.83	4.45	994.00	5.65	469.90
Mean	–	–	6.82	664.56	429.58	40.26	57.77	2.34	2.57	176.37	2.21	148.07
SD	–	–	0.15	317.62	200.31	5.59	5.40	0.40	0.59	182.04	1.23	75.37
Samples exceeding standards	–	–	–	3	6	–	–	–	–	4	–	–

BW bore well, *DW* dug well, all concentrations in mg/L except EC (µS/cm) and pH (no unit), S_i standard prescribed by NSDWQ guidelines

flank. In general, the groundwater in Ogun Waterside is relatively better during the wet season when compared to the dry season. This may be due to high rate of groundwater extraction during dry season and the associated groundwater flow inversion from the sea towards aquifers that are hydraulically connected with the sea (Fig. 7).

Inclusive interpretation of the integrated approach

This study involves an integrated approach comprising geophysical and hydrochemical methods in which the hydrochemical analysis was used to juxtapose the result of the

Table 3 Results of the physical and chemical contents of groundwater sample analyzed for the dry season (modified after Badmus et al. 2020, p. 4)

Sample no.	Sample location	Source type	pH	EC	TDS	Na^+	K^+	Mg^{2+}	Ca^{2+}	Cl^-	SO_4^{2-}	HCO_3^-
S-1	Ilusin	BW	6.80	619.17	396.27	37.40	64.65	3.50	2.12	106.30	1.8	180.50
S-2	Ibiade	DW	5.16	703.80	450.43	46.78	71.25	2.87	4.13	177.50	3.5	144.40
S-3	Oni	BW	5.06	730.17	467.31	64.91	71.81	3.43	2.93	248.30	3.83	72.10
S-4	Ebute-Oni	DW	4.95	561.77	359.53	62.15	72.42	3.40	3.41	142.00	3.95	72.20
S-5	Ologumeta	DW	5.81	453.38	290.16	57.46	78.40	3.31	3.74	71.30	3.85	72.10
S-6	Iwopin	DW	5.96	574.95	367.97	56.44	84.40	3.25	3.83	142.00	5.75	72.30
S-7	Alo	BW	4.95	613.58	392.69	61.80	68.50	3.61	3.23	177.40	5.85	72.30
S-8	Igele	BW	6.82	726.00	464.64	48.88	74.70	3.51	3.70	106.50	10.8	216.55
S-9	Akila	BW	6.64	658.80	421.63	44.70	80.95	2.95	3.67	142.00	2.91	144.45
S-10	Agodo	DW	4.70	580.28	371.38	44.80	66.65	2.96	3.87	142.00	2.7	108.40
S-11	Lokula	BW	4.78	586.58	375.41	43.80	70.45	3.76	3.89	177.40	3.61	72.50
S-12	Igbafowo	BW	5.29	631.16	403.94	45.75	64.20	3.22	2.25	177.70	2.42	108.40
S-13	Abigi	BW	4.68	736.03	471.06	44.65	57.70	3.47	4.53	248.60	3.56	108.55
S-14	Araromi Obu	BW	6.73	1230.72	787.66	35.83	61.77	2.73	2.11	213.50	1.82	469.90
S-15	Ayede	BW	6.80	506.00	323.84	35.73	64.92	3.53	2.94	71.00	1.72	144.00
S-16	Ayila	BW	6.63	660.38	422.64	34.13	60.75	2.80	1.93	177.40	1.23	144.40
S-17	Itebu Elero	DW	6.73	461.14	295.13	62.15	72.42	3.40	3.41	77.60	3.95	72.20
S-18	Ayesan	DW	6.73	714.56	457.32	30.45	60.82	3.73	2.82	213.50	1.6	144.40
S-19	Lomiro	BW	6.88	674.75	431.84	41.55	60.80	2.93	2.74	213.80	1.62	108.40
S-20	Ibu	BW	6.85	617.73	395.35	40.85	62.75	2.80	1.84	177.20	1.51	108.40
S-21	Iyemoje	DW	5.36	588.73	376.79	43.60	68.69	3.61	4.74	177.10	6.75	72.30
S-22	Efire	BW	5.38	627.73	401.75	43.65	59.75	3.75	4.87	177.40	3.78	108.55
S-23	Imakun-Omi	BW	7.19	3909.47	2502.06	47.55	61.40	3.62	3.89	2166.00	2.95	216.65
S-24	Ita Otu	BW	5.15	659.09	421.82	48.72	70.85	3.41	3.81	213.80	8.93	72.30
S-25	Tigara	BW	5.25	474.59	303.74	45.60	68.91	3.85	3.93	106.50	2.75	72.20
S-26	Irokun	DW	5.93	1409.28	901.94	44.70	64.25	3.46	2.36	640.30	2.47	144.40
S-27	Igbo-edun	DW	6.62	582.41	372.74	47.90	64.75	3.75	2.14	142.30	3.40	108.50
S-28	Eba	DW	6.45	458.86	293.67	48.55	57.76	2.89	2.14	71.30	2.53	108.50
S-29	Isekun	DW	5.80	1802.67	1153.71	47.65	61.82	4.23	2.13	852.40	3.88	181.60
S-30	Ode-Omi	DW	6.65	1185.89	758.97	45.60	61.15	4.17	2.34	532.60	4.61	108.50
S_i	–	–	8.5	1,000	500	200	–	0.2	–	250	100	–
Min	–	–	4.68	374.59	290.16	30.45	57.70	2.73	1.84	71.00	1.23	72.10
Max	–	–	7.19	3909.47	2502.06	64.91	84.40	4.23	4.87	2166.00	10.80	469.90
Mean	–	–	5.96	821.32	527.78	46.79	66.99	3.40	3.18	276.09	3.67	127.67
SD	–	–	0.81	648.92	412.51	8.40	6.66	0.39	0.88	388.97	2.12	76.23

Table 3 (continued)

Sample no.	Sample location	Source type	pH	EC	TDS	Na$^+$	K$^+$	Mg^{2+}	Ca^{2+}	Cl$^-$	SO$_4$$^{2-}$	HCO$_3$$^-$
Samples exceeding standards	–	–	–	5	5	–	–	–	–	4	–	–

BW bore well, *DW* dug well, all concentrations in mg/L except EC (µS/cm) and pH (no unit), S_i standard prescribed by NSDWQ guidelines

geophysical survey. The ERT models generally revealed low-to-high resistivity values across the study area. Low-resistivity layer (typical of brackish/saline water intruded layer) was delineated in Imakun-omi, Irokun, Isekun, and Ode-omi. These locations correspond to areas where high chloride concentration, electrical conductivity, total dissolved solids, and high equivalent salinity values were recorded from the water sample physico-chemical analysis. Most elevated chloride values (usually above 250 mg/L) obtained at these locations attest to the invasion by brackish/saltwater as reflected by the low-resistivity values in the ERT inversion model for these locations. This is more evident during the dry season which may be attributed to low precipitation and exacerbated by high rate of groundwater withdrawal. Also, the presence of high resistivity signature in locations like Iwopin, Itebu-elero, and Ayila is suggestive of possible presence of high-quality freshwater. These locations also correspond to zones where chloride concentration, electrical conductivity, and total dissolved solids within accepted limits were recorded. Thus, the results of the hydrochemical analysis corroborate and agree with the results of the geophysical survey suggesting saltwater intrusion in locations such as Imakun-omi, Irokun, Isekun, and Ode-omi.

Conclusion

Groundwater quality in Ogun Waterside has been substantiated using integrated geophysical and hydrochemical methods. The ERT imaging penetrated a depth range of 37 m–197 m below the ground surface. The ERT inversion model was able to map the saltwater intrusion zones in the study site. Low-resistivity signatures generally below 20 Ωm were delineated in Imakun-omi, Irokun, Isekun, and Ode-omi. The result revealed vivid evidence of vertical and lateral migration of saltwater into the coastal groundwater aquifer in the southern part of the study area.

The physicochemical analysis also revealed high TDS, EC, and Cl concentrations in the southern part (Imakun-omi, Isekun, Irokun, and Ode-omi) of the study area. This corroborates the ERT result and clearly indicates that the aquifers in these locations have been polluted by saline water. There is a general increase in the ionic concentrations from wet to dry season which may be ascribed to difference in hydraulic head caused by low precipitation and possibly aggravated by high rate of groundwater withdrawal during the dry season. This implies that the groundwater in Ogun Waterside is relatively poor in the dry season and may be unsuitable for consumption without proper treatment.

The computed WQI values range from 35.19 to 141.72 in the wet season and from 38.6 to 266.79 in the dry season. The high chloride content noticed in samples taken
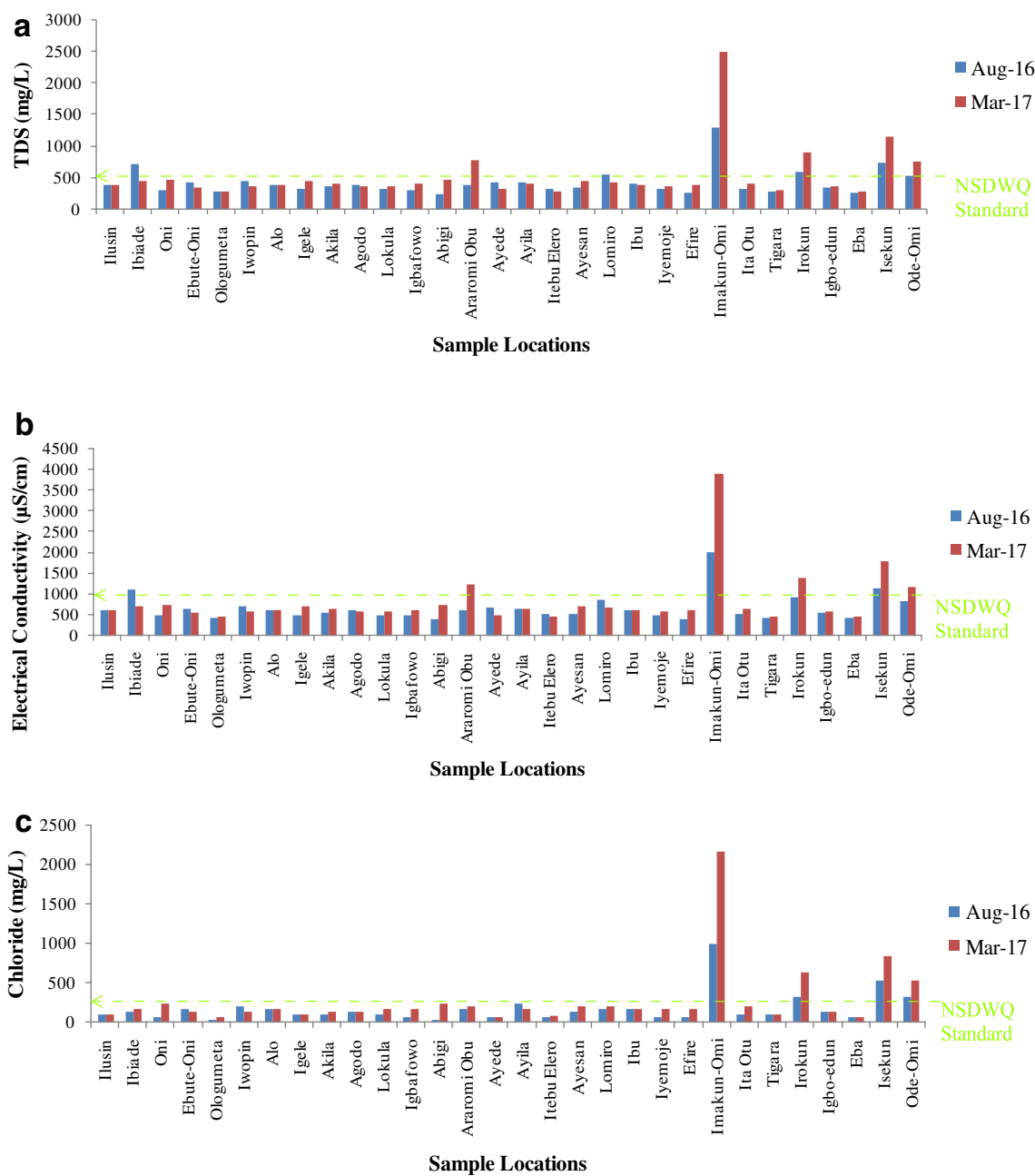
Fig. 6 NSDWQ threshold limit against (**a**) TDS, (**b**) EC, and (**c**) Cl concentrations in water samples during wet season (Aug-16) and dry season (Mar-17)

towards the southern flank was responsible for high WQI values reported in Ogun Waterside. The WQI revealed that the groundwater taken from Imakun-omi was found to be poor during wet season, while samples taken from Isekun and Irokun were found to be poor and the sample taken from Imakun-omi was found to be very poor (unsuitable) for drinking during dry season.

Based on the obtained results from the ERT survey and analyzed hydrochemical data, it is concluded that there is an enhanced thread of saltwater intrusion into the coastal groundwater aquifer of Imakun-omi, Irokun, Isekun, and Ode-omi during the dry season. It is, therefore, recommended that proper monitoring and mitigation practice need be initiated immediately by the concerned Government agencies to curb further deterioration.
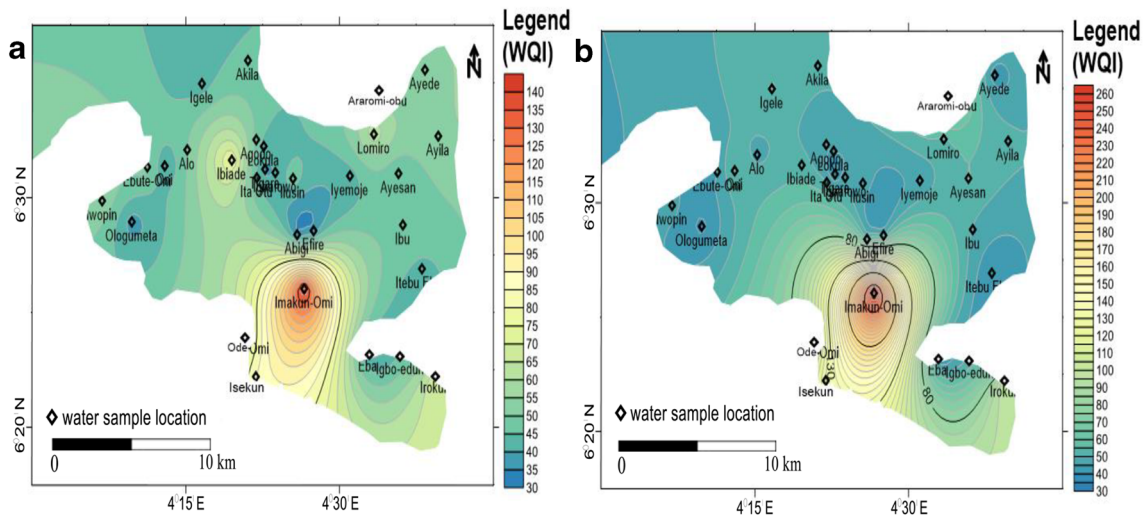
Fig. 7 Map showing water quality index in Ogun Waterside during (**a**) wet season (Aug-16) (**b**) dry season (Mar-17)

Table 4 Seasonal variation of WQI for samples in Ogun Waterside

Sample location	Wet season WQI	Water type	Dry season WQI	Water type
Ilusin	48.32	Excellent	48.56	Excellent
Ibiade	76.13	Good	52.69	Good
Oni	40.41	Excellent	56.08	Good
Ebute-Oni	52.14	Good	44.71	Excellent
Ologumeta	37.44	Excellent	38.60	Excellent
Iwopin	55.05	Good	46.82	Excellent
Alo	49.92	Excellent	48.21	Excellent
Igele	42.20	Excellent	55.41	Good
Akila	46.32	Excellent	51.68	Good
Agodo	48.51	Excellent	44.49	Excellent
Lokula	42.53	Excellent	45.76	Excellent
Igbafowo	40.53	Excellent	48.69	Excellent
Abigi	35.19	Excellent	54.94	Good
Araromi Obu	49.49	Excellent	83.62	Good
Ayede	51.68	Good	41.72	Excellent
Ayila	54.33	Good	51.52	Good
Itebu Elero	43.61	Excellent	40.56	Excellent
Ayesan	45.22	Excellent	55.36	Good
Lomiro	63.67	Good	53.71	Good
Ibu	50.19	Good	49.80	Excellent
Iyemoje	42.16	Excellent	46.78	Excellent
Efire	36.25	Excellent	48.79	Excellent
Imakun-Omi	141.72	Poor	266.79	Very Poor
Ita Otu	43.43	Excellent	51.21	Good
Tigara	38.91	Excellent	39.07	Excellent
Irokun	69.55	Good	100.51	Poor
Igbo-edun	45.95	Excellent	47.48	Excellent
Eba	37.36	Excellent	38.96	Excellent
Isekun	85.09	Good	125.94	Poor
Ode-Omi	63.83	Good	87.56	Good

References

Abdalla OA, Ali M, Al-Higgi K, Al-Zidi H, El-Hussain I, Al-Hinai S (2010) Rate of seawater intrusion estimated by geophysical methods in an arid area: Al Khabourah. Oman Hydrogeol J 18(6):1437–1445

Abd-Elhamid HF, Javadi AA, Qahman KM (2015) Impact of over-pumping and sea level rise on seawater intrusion in Gaza aquifer (Palestine). J Water Clim Change 6(4):891–902

Adebo B (2012) Assessment of saline intrusion in Lagos coastal aquifer. Int Arch Appl Sci Technol IAAST 3(3):23–28

Adeoti L, Alile OM, Uchegbulam O (2010) Geophysical investigation of saline water intrusion into freshwater aquifers: a case study of Oniru. Lagos State Sci Res Essays 5(3):248–259

Adepelumi AA, Ako BD, Ajayi TR, Afolabi O, Omotoso EJ (2009) Delineation of saltwater intrusion into the freshwater aquifer of Lekki Peninsula, Lagos. Nigeria Environ Geol 56(5):927–933

Adeyemo IA, Omosuyi GO, Adelusi AO (2017) Geoelectric soundings for delineation of saline water intrusion into aquifers in part of eastern Dahomey basin, Nigeria. J Geosci Environ Protection 5(3):213–232. https://doi.org/10.4236/gep.2017.53015

Adeyemo IA, Omosuyi OG, Adelusi AO (2015) Hydrochemical investigation of saline water intrusion into aquifers in part of Eastern Dahomey Basin, Southwestern Nigeria. J Environ Earth Sci 5(11):138–153

AGI (2003) Earth Imager 2-D resistivity inversion software, version 1.5.10. Advanced Geosciences, Inc., Austin, TX, US.

Aizebeokhai AP (2010) 2D and 3D geoelectrical resistivity imaging: Theory and field design. Sci Res Essays 5(23):3592–3605

APHA (1995) Standard methods for the examination of water and waste water, 17th edn. American Public Health Association, Washington

Ayolabi EA, Enoh IJ, Folorunso AF (2013a) Engineering site characterisation using 2-D and 3-D electrical resistivity tomography. Earth Sci Res 2(1):133–142

Ayolabi EA, Folorunso AF, Odukoya AM, Adeniran AE (2013b) Mapping saline water intrusion into the coastal aquifer with geophysical and geochemical techniques: the University of Lagos campus case (Nigeria). SpringerPlus 2(1):420–433. https://doi.org/10.1186/2193-1801-2-433

Ayolabi EA, Folorunso AF, Kayode OT (2013c) Integrated geophysical and geochemical methods for environmental assessment of municipal dumpsite system. Int J Geosci 850–862. https://doi.org/10.4236/ijg.2013.45079

Badmus GO, Akinyemi OD, Gbadebo AM, Oyedepo JA (2020) Hydrochemical analysis of groundwater quality along the coastal aquifers in part of Ogun Waterside, Ogun State, southwestern Nigeria. Heliyon 6(12):1–12. https://doi.org/10.1016/j.heliyon.2020.e05661

Batabyal AK, Chakraborty S (2015) Hydrogeochemistry and water quality index in the assessment of groundwater quality for drinking uses. Water Environ Res 87(7):607–617

Billman HG (1992) Offshore stratigraphy and paleontology of dahomey Embayment, West Africa. Nigerian. Association Petrol Explorationist Bull 7(2):121–130

Darnault CJ, Godinez IG (2008) Coastal aquifers and saltwater intrusion. Overexploitation and contamination of shared groundwater resources: management, (Bio) Technological, and Political Approaches to Avoid Conflicts 185–201.

Fakolade OR, Obasi RA (2012) The geochemical assessment of subsurface coastal plain clastic deposits of eastern dahomey basin around Lagos area, south-west. Nigeria J Sci Technol 1(6):300–307

Goebel M, Pidlisecky A, Knight R (2017) Resistivity imaging reveals complex pattern of saltwater intrusion along Monterey coast. J Hydrol 551:746–755. https://doi.org/10.1016/j.jhydrol.2017.02.037

Gurunadha Rao VVS, Tamma Rao G, Surinaidu L, Rajesh R, Mahesh J (2011) Geophysical and geochemical approach for seawater intrusion assessment in the Godavari Delta Basin, AP, India. Water Air Soil Pollut 217(1–4):503–514

Hodlur GK, Dhakate R, Sirisha T, Panaskar DB (2010) Resolution of freshwater and saline water aquifers by composite geophysical data analysis methods. Hydrol Sci J-Journal des Sciences Hydrologiques 55(3):414–434

Idowu AA, Olaoye OJ, Ifegbesan A, Abdul WO, Olawale OB (2012) Evaluation of fishermen and fish traders in transactional sex for fish marketing in coastal areas of Ogun waterside local government area, Ogun State, Nigeria. Global J Sci Front Res Agric Biol 12(1):42–54

Jones HA, Hockey RD (1964) Geology of parts of South-western Nigeria. Bull Geol Surv Nigeria 31:56–77

Nigerian Industrial Standard for Drinking Water Quality (2007) Nigeria Industrial Standard, Approve by Standard Organization of Nigeria Governing Council. ICS 13. 060. 20, pp 15–19.

Nowroozi AA, Horrocks SB, Henderson P (1999) Saltwater intrusion into the freshwater aquifer in the eastern shore of Virginia: a reconnaissance electrical resistivity survey. J Appl Geophys 42(1):1–22

Obaje NG (2009) Geology and mineral resources of Nigeria. Published by Springer-Verlag, Berlin Heidelberg, p 221p

Odebiyi OC, George FO, Olaoye OJ, Idowu AA, Agbonlahor MU, Oke AO (2013) Economic analysis of coastal fisheries value chain development in Ogun Waterside Local Government Area, Ogun State, Nigeria. J Agric Econ Dev 2(9):345–355

Olabode SO (2015) Subsidence patterns in the Nigerian sector of Benin (Dahomey) Basin: evidence from three offshore wells. Ife J Sci 17(2):455–475

Olaoye OJ, Idowu AA, Omoyinmi GAK, Akintayo IA, Odebiyi OC, Fasina AO (2012) Socio-economic analysis of artisanal fisher folks in ogun water-side local government areas of Ogun State, Nigeria. Global J Sci Front Res Agric Biol 12(4):9–22

Omatsola ME, Adegoke OS (1981) Tectonic evolution and Cretaceous stratigraphy of the Dahomey basin. Nigeria J Min Geol 18(1):130–137

Oyedele KF, Momoh EI (2009) Evaluation of Sea water Intrusion in freshwater aquifers in a Lagoon Coast: a case study of the University of Lagos Lagoon, Akoka. Nigeria Rep Opin 1(2):61–72

Oyeyemi KD, Aizebeokhai AP, Oladunjoye MA (2015) Integrated Geophysical and Geochemical investigations of saline water intrusion in a coastal alluvial terrain, Southwestern Nigeria. Int J Appl Environ Sci 10(4):1275–1288

Publisher's Note Springer Nature remains neutral with regard to jurisdictional claims in published maps and institutional affiliations.